

## Plasticity-Fractal-Behavior Trends for Different Aluminum Alloys Tested in Tension

O. A. Hilders<sup>1</sup>, M. Ramos<sup>1</sup>, N. D. Peña<sup>1</sup>, L. Sáenz<sup>2</sup>, R. A. Caballero<sup>1</sup>

<sup>1</sup>School of Metallurgical Engineering & Materials Science, Central University of Venezuela (UCV),  
Apartado 47514, Caracas, 1041-A, Venezuela

<sup>2</sup>Department of Materials and Fabrication Processes, University of Carabobo (UC),  
Apartado 3155, Valencia, 2002, Venezuela

Keywords: Fractal Dimension, Fractal Geometry, Quantitative Fractography, Fracture Surface Morphology.

### Abstract

Several results on fracture surface morphology and its relation with the plastic strain to cause tensile fracture have been obtained for 13 aluminum alloys. When the dimple size  $d_T$ , or the true fracture strain  $\epsilon_f$  are related with the fractal dimension  $D$ , the same general trend is obtained:  $D$  increases as  $\epsilon_f$  or  $d_T$  decrease in a first step. Once  $D$ ,  $\epsilon_f$  and  $d_T$  reached a critical value, the variation is reversed and the fractal dimension decreases as  $\epsilon_f$  and  $d_T$  continue to fall. The overall data were compiled in two general curves, both of the twin reversed "C"-shaped type. From the later, it was demonstrated that  $\epsilon_f$  is a direct function of  $D$ , i.e. the higher the true fracture strain, the higher the fractal dimension.

### 1. Introduction

In recent years, the quantitative characterization of fracture surfaces has been attracting growing interest, although many authors agree that the complex patterns exhibited by rough surfaces are better described in terms of *fractal geometry* rather than the euclidean geometry [1-7]. The former approach provides an intrinsic roughness index called *fractal dimension*  $D$  [8-10], an intensive property which gives information about the structure of the surface. In many cases the properties of materials has been correlated to the measured *fractal dimension* [11-17]. For aluminum alloys some works are related to: the corrosion cracking behavior of 7076/T6 ternary Al-Mg-Zn alloy [18], the analysis of different aluminum alloys reinforced with particulate SiC fractured in the fatigue test [19], the fractal dimension dependence of crack size tolerance index of several 7000-series aluminum alloys [20], the superplasticity of 7475 Al alloy [21], the study of the fatigue fracture surface of several particulate SiC/Al composites, as related with the plastic amplitude and the fatigue life [22], etc.

This article gives a survey of the results of a study in the field of quantitative fractography applied to 13 different aluminum alloys, to develop a relation between the plasticity and the

fractal characteristics of tension fracture surfaces. Although a functional form of the *fractal dimension* dependence of the fracture toughness has been developed for several aluminum alloys [23], the relationship between the strain required to cause fracture, the microfracture morphology and the *fractal dimension* is not clear yet. Then, we intend to develop this kind of relationship through the examination of the fine-scale topography of fractured surfaces and their connection with the true fracture strain and the fractal characteristics of the tension fracture surfaces.

## 2. Experimental Procedure

The materials used in this work consisted of three nominal 7000 Al alloys, namely, 7178/T651, 7475/T7351 and 7050/T7451; two nominal 2000 Al alloys, the 2024/T351 and the 2090/T8; four 7075/T651 Al alloys with different Zn/Mg ratios, an Al-0.57Si-2.03Ge alloy (wt. %) aged for 24h at 403 K and three Al-Mg-Si alloys with different Li content: 1.52, 1.75 and 2.09 (wt. %), the three of them aged for 100 h at 433 and 453 K. The chemical compositions of the studied alloys are given in Table 1. The Al-Mg-Si (-Li) alloys were prepared and tested according to the procedure presented in the companion paper. The experimental procedures for the rest of the alloys, including tensile tests and fractography, were conducted as reported elsewhere [11,23], although all the fractal dimension measurements were performed using just the slit island method. The method based on the “mean chord in space” (24-27), was used to calculate the average dimple size.

Table 1: Chemical Composition (wt. %) of the Studied Alloys.

Alloy Designation	Zn	Mg	Cu	Cr	Fe	Si	Ti	Mn	Zr	Li	Ge
7075/T651	5.62	2.48	1.60	0.22	0.010	0.010					
7075/T651	6.62	2.74	1.59	0.21	0.015	0.020	0.020				
7075/T651	7.63	2.74	1.55	0.24	0.100	0.220	0.010				
7075/T651	7.86	2.79	1.55	0.21	0.100	0.257	0.010				
7178/T651	6.80	2.70	2.00	0.30	0.450	0.390					
7475/T7351	5.80	2.30	1.65	0.23	0.093	0.051	0.040	0.02			
7050/T7451	6.30	2.30	2.40	0.03	0.130	0.110	0.030	0.08	0.12		
2024/T351		1.52	4.10		0.110	0.050		0.54			
2090/T8			2.34		<0.10		0.020		0.12	2.13	
Al-Mg-Si-1.52Li		0.65		0.20	0.072	0.820				1.52	
Al-Mg-Si-1.75Li		0.65		0.20	0.080	0.790				1.75	
Al-Mg-Si-2.09Li		0.64		0.21	0.025	0.840				2.09	
Al-Si-Ge						0.570					2.03

## 3. Results and Discussion

The experimental data for the aluminum alloys were analyzed according to the twin-reversed “C”-shaped curves presented in Figures 1 and 2, which show the dependence of the true fracture strain and dimple size on the fractal dimension. It can be seen in Figure 1 that as soon as the ductility decreases, the fractal dimension increases, but for a small enough

values of  $\epsilon_f$ , however, this tendency is reversed and the fractal dimension decreases. This behavior can be explained as follows: when the ductility falls, the dimple size decreases, but the dimples themselves become deeper. As a result of this process, the tortuosity of the fracture surfaces increases and so the fractal dimension. When a certain critical value of  $\epsilon_f$  is reached, the fractal dimension starts to decrease as the ductility continues to fall, since the edges around the dimples become shallow as the lack of plasticity opposed its growth, increasing the fracture surface flatness. As can be seen in Figure 1, the experimental data corresponding to the 13 aluminum alloys are closely distributed around the twin-reversed “C”-shaped curves which are extended into a range of fractal dimension values. There is not an apparent explanation for this behavior nor for the kind of alloys associated to each curve. The critical value of the true fracture strain,  $\epsilon_{fc} \approx 24.25\%$ , is related with two critical values of the fractal dimension,  $D_{c1} = 1.18$  and  $D_{c2} = 1.25$ , which in turn are associated with the inner and the outer curves respectively.

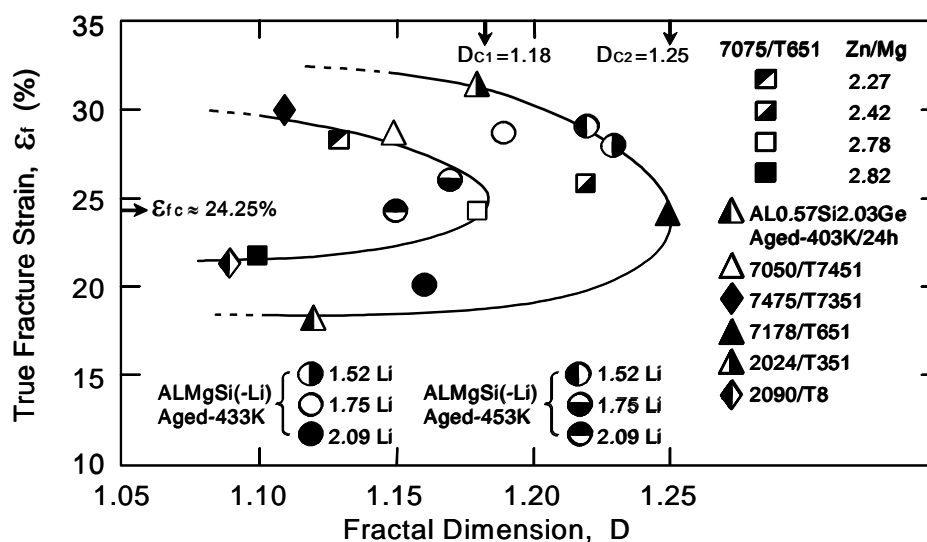


Figure 1: Twin reversed “C”-shaped curves for the dimple size/fractal dimension relationship.

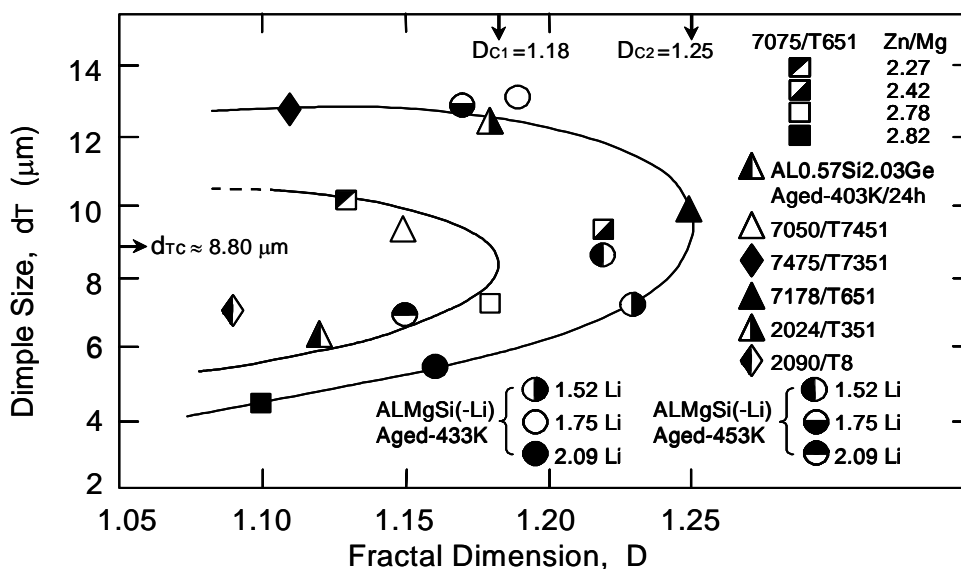


Figure 2: Twin reversed “c”-shaped curves for the true fracture strain/fractal dimension relationship.

The similarity between the Figure 1 and that of the dimple size vs fractal dimension (Figure 2) are at once apparent, since there is a direct relation between ductility and dimple size, but there are, nevertheless, some differences. Among the later is the presence of a less defined value of a critical dimple size  $d_T$ , as compared with the good definition showed by

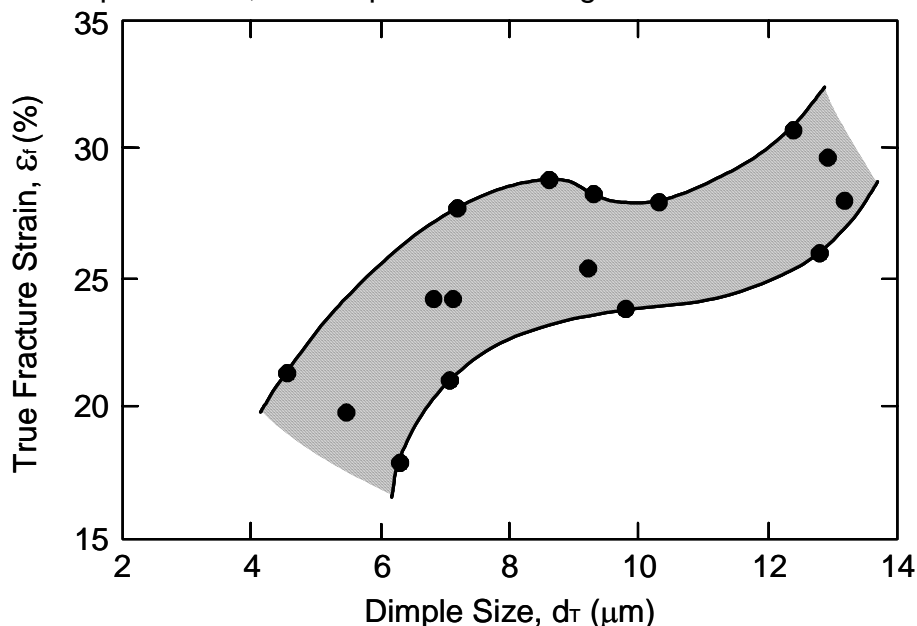


Figure 3: The relationship between the true fracture strain and the dimple size.

$\epsilon_{fC}$  in Figure 1. In despite of this fact, for  $d_{TC} \approx 8.80 \mu\text{m}$  the values of  $D_{C1}$  and  $D_{C2}$  in Figure 2 are the same of that developed for Figure 1, corresponding very close to the nose of the curves. A second difference is obviously related with the distribution of the experimental data which changes according to the particular value of the dimple size. Although very complex, the general dependence of the ductility on the dimple size can be described as a direct relation, i.e. the higher the true fracture strain the higher the dimple size.

Table 2: True Fracture Strain, Dimple Size and Fractal Dimension Data.

Alloy Designation	$\epsilon_f$ (%)	$d_T$ ( $\mu\text{m}$ )	D
2024/T351	31.20	12.31	1.18
7475/T7351	30.00	12.82	1.11
Al-Mg-Si-1.52Li. Aged 25h/453K	29.10	8.51	1.22
7050/T7451	28.50	9.21	1.15
Al-Mg-Si-1.75Li. Aged 100h/433 K	28.40	13.11	1.19
7075/T651. Zn/Mg = 2.27	28.20	10.16	1.13
Al-Mg-Si-1.52Li. Aged 100h/433 K	28.00	7.10	1.23
Al-Mg-Si-1.75Li. Aged 25h/453 K	26.00	12.82	1.17
7075/T651. Zn/Mg = 2.42	25.70	9.14	1.22
7075/T651. Zn/Mg = 2.78	24.30	7.02	1.18
Al-Mg-Si-2.09Li. Aged 25h/453 K	24.30	6.75	1.15
7178/T651	24.00	9.73	1.25
7075/T651. Zn/Mg = 2.82	21.70	4.45	1.10
2090/T8	21.20	7.12	1.09
Al-Mg-Si-2.09Li. Aged 30h/433 K	20.00	5.43	1.16
Al-Si-Ge. Aged 24h/403 K	18.00	6.20	1.12

This relation can be seen in Figure 3, which shows a band of variation instead of a single curve. Table 2 shows ordered data from high to low values of  $\varepsilon_f$  and the corresponding data of  $D$  and  $d_T$ . On the other hand, several typical morphologies associated to the same mechanism of fracture (micro-void coalescence), can be seen in Figure 4. The morphologies ranged as irregular, tearing, equiaxed and elongated well defined voids (Figs. 4-a, b, c and d respectively).

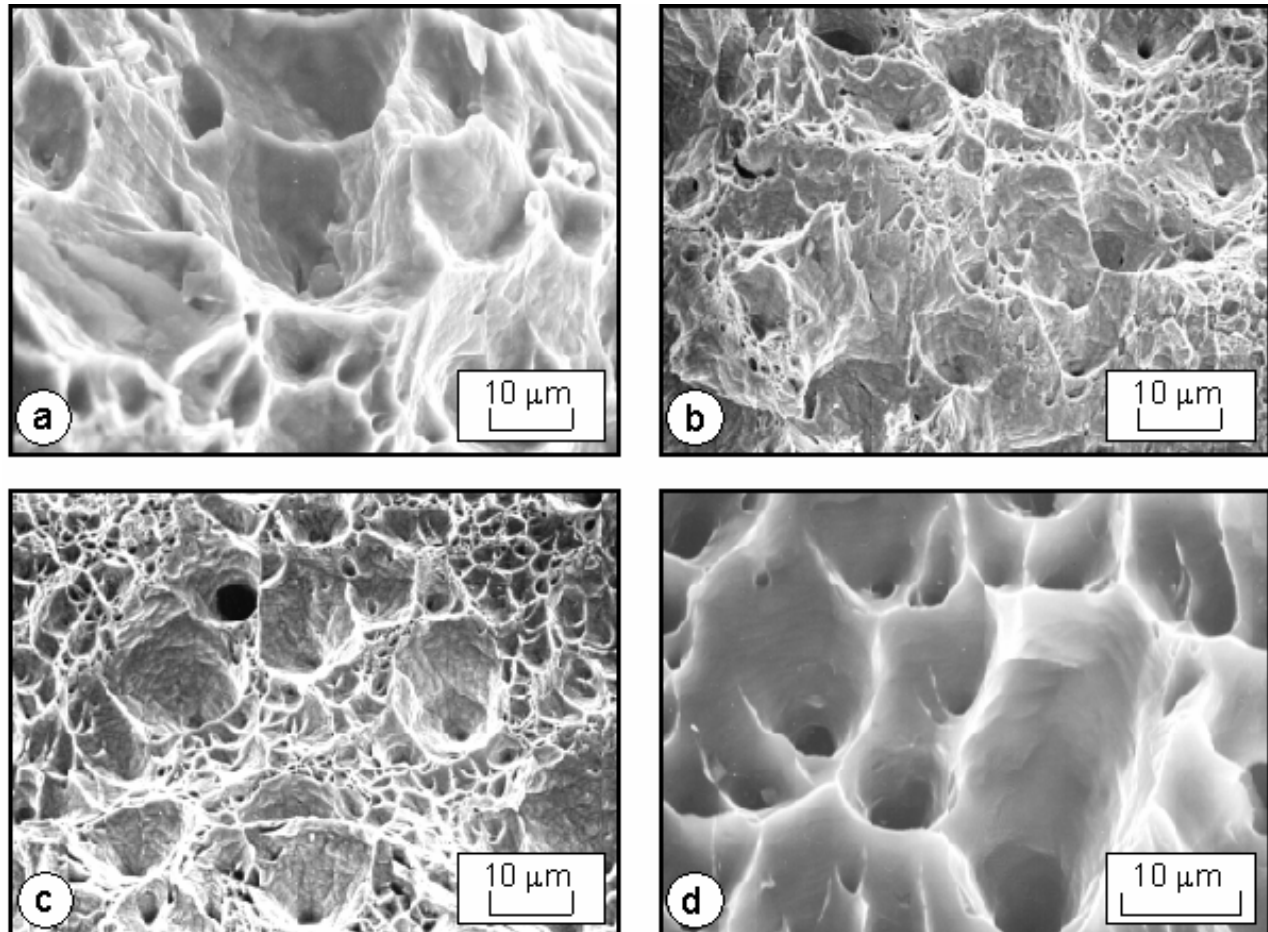


Figure 4: SEM fractographs of some of the studied aluminum alloys. (a) 7475/T7351; (b) 7178/T651; (c) 7050/T7451 and (d) 7075/T651 (Zn/Mg = 2.42).

#### 4. Conclusions

A relationship between the strain required to cause fracture in tension, the micro-void coalescence morphology and the fractal dimension has been developed for 13 different aluminum alloys. Both, the relation between the ductility and the fractal dimension, on one hand, and between the dimple size and the fractal dimension, on the other hand, are represented by two curves for each case. These curves are of the twin reverse “C”-shaped type and represent the changes in the fractal characteristics as a function of the plastic behavior:  $D$  increases as  $\varepsilon_f$  or  $d_T$  decrease in a first step. Once  $D$ ,  $\varepsilon_f$  and  $d_T$  reached a critical value, the variation is reversed and the fractal dimension decreases as  $\varepsilon_f$  and  $d_T$  continue to fall. It was

observed that the ductility increases as the dimple size increases, although this relation shows a wide band of variation.

### Acknowledgements

The authors would like to thank the financial support of the Venezuelan National Found of Science and Technology (FONACIT) through the Project N° S1-2000000556.

### References

- [1] H.J. Herrmann, *Fractals and Disordered Systems*, Springer, Berlin, 1991.
- [2] R.H. Dauskardt, F. Haubensak and R.O Ritchie, *Acta Metall. Mater.*, 38, 143-159, 1990.
- [3] H. Su and Z. Yan, *Mater. Lett.*, 13, 102-104, 1992.
- [4] A.M. Brandt and G. Prokopski, *J. Mater. Sci.*, 28, 4762-4766, 1993.
- [5] W. Lei and B. Chen, *Eng. Fract. Mech.*, 50, 149-155, 1995.
- [6] A.S. Balankin, *Phil. Mag. Lett.*, 74, 415-422, 1996.
- [7] L.R. Botvina, A.V. Ioffe and T.V. Tetyueva, *Met. Sci. & H. Treat.*, 39, 296-300, 1997.
- [8] B.B. Mandelbrot, D.E. Passoja and A.J. Paullay, *Nature*, 308, 721-722, 1984.
- [9] B.B. Mandelbrot, *Comp. Rend.*, 288A, 81-83, 1979.
- [10] G. Caldarelli, C. Castellano and A. Vespignani, *Phys. Rev. E.*, 49, 2673-2679, 1994.
- [11] O.A. Hilders, *Aluminum Alloys Their Physical and Mechanical Properties*, edited by T. Sato, S. Kumai, T. Kobayashi and Y. Murakami, The Japan Institute of Light Metals, Tokyo, 955-960, 1998.
- [12] C.H. Shek, G.M. Lin, J.K.L. Lai and Z.F. Tang, *Metall. Mater. Trans. A*, 28A, 1337-1340, 1997.
- [13] E. Hornbogen, *Int. Mater. Rev.*, 34, 277-296, 1989.
- [14] X.G. Jiang, W.Y. Chu and C.M. Hsiao, *Acta Metall. Mater.*, 42, 105-108, 1994.
- [15] O.A. Hilders, N. Peña, M. Ramos, L. Berrío y L. Sáenz, *Mater. Sci. Forum*, 331-337, 1273-1278, 2000.
- [16] O.A. Hilders, L. Sáenz, M. Ramos and N.D. Peña, *J. Mater. Eng. Perf.*, 8, 8-11, 1999.
- [17] M. Tanaka and H. Lizuka, *Z. Metallkde.*, 82, 442-447, 1991.
- [18] V.K. Horvath and H.J. Herrmann, *Chaos Solitons Fractals*, 1, 395-402, 1991.
- [19] D.L. Davidson, *J. Mater. Sci.*, 24, 681-687, 1989.
- [20] O.A. Hilders, N.D. Peña, M. Ramos, L. Sáenz, L. Berrío, R.A. Caballero and A. Quintero, *Mater. Sci. Forum*, 396-402, 1411-1416, 2002.
- [21] J. Xinggang, C. Jianzhong and M. Longxiang, *J. Mater. Sci. Lett.*, 12, 1616-1618, 1993.
- [22] X.W. Li, J.F. Tian, N.L. Han, Y. Kang and Z.G. Wang, *Mater. Lett.*, 29, 235-240, 1996.
- [23] O.A. Hilders, *J. Mater. Proc. Tech.*, Special Issue, 117/3, CDROM Sec. A4, 2001.
- [24] J.L. Chermant and M. Coster, *J. Mater. Sci.*, 14, 509-534, 1979.
- [25] O.A. Hilders and M.G. Santana, *Metallography*, 21, 151-164, 1988.
- [26] O.A. Hilders, *Applications of Stainless Steel 92*, edited by H. Nordberg and J. Björklund, ASM International, Stockholm, 1017-1027, 1992.
- [27] O.A. Hilders and N.D. Peña, *Adv. Perf. Mater.*, 4, 49-61, 1997.